# 2nd QUARTERLY PROJECT STATUS REPORT

Project Title:
Effects of Calcium Magnesium Acetate on the Combustion of Coal-Water Slurries

DOE/PC/89776--T7

DE92 018314

DOE Grant #: DE-FG22-89PC89776

Project Period: 1 December 1989 - 28 February 1990

## Project Objectives:

The general objective of the project is to investigate the combustion behavior of single Coal-Water Slurry particles burning at high temperature environments. Both uncatalyzed as well catalyzed CWS drops with Calcium Magnesium Acetate (CMA) catalyst will be investigated. Emphasis will also be given in the effects of CMA on the sulfur capture during combustion. To help achieve these objectives the following project tasks were carried over this *2nd* three month period.

## Project Tasks:

1 **PURCHASE OF SLURRIES AND CONSTRUCTION OF SLURRY AGITATION APPARATUS** A micronized and beneficiated coal water slurry was purchased from *Oiisca* for the needs of this study. This slurry contains 50% solids (bituminous coal) of mean particle size of 20 $\mu$m. In the solids the ash content is 0.94%, the sulfur content 0.86%, fixed carbon is 61.6% and volatiles 37%. The mixture also contains a total of 1% ammonium lignosulfonate as a surfactant. The slurry sediments within 8 hrs, therefore, to prevent sedimentation an apparatus was constructed to continuously tumble bottles of slurry, at slow speed, using a small motor, Fig. 1.

2 **CONSTRUCTION OF A WATER-COOLED PARTICLE PROBE** A water-cooled particle probe, 60 cm long, 2.3 cm inner diameter, 5.4 cm outer diameter, was constructed out of four concentric stainless steel tubes. The outer three constitute

## DISCLAIMER

the cooling jacket and in the annulus between the inner two tubes inert gas fl ows to quench the combustion reactions. The topmost four inches of the innermost tube are perforated to enable the inert gas to flow to the top of the probe. The design specifications of the probe and the determination of the required cooling water flowrate took into account the heating load in the furnace as well as the water pressure drop in the annulus. Heat shield insulation rings were machined out of a low density alumina plate purchased from *Zircar* and glued on the probe with high-temperature alumina glue (*Zircar*). The overall, outside diameter of the probe resulted to 6.0 cm. The collection probe was then mounted on a translation stage driven by a small (1/75 HP) dc motor. The whole assembly, shown in Fig. 2, can be easily moved in position below the furnace and can reach any axial position inside the radiation cavity.

**3 SUCTION THERMOMETRY** While furnace wall temperatures were monitored by type *B* thermocouples attached to the wall, gas temperatures inside the furnace were measured by a suction thermometer, shown in Figs. 3 and 4 . This instrument utilized a type *S* thermocouple in a sheath inside a 0.9 cm i.d., 57 cm long, high density alumina tube. The thermocouple junction was placed at a distance of 2 cm from the top end. The bottom end of the alumina tube was attached to a pump to provide suction. Low density alumina blanket was inserted between the thermocouple sheath and the tube to serve as a radiation shield for the thermocouple tip. The pump suction drove furnace gases around the thermocouple junction through the permeable blanket in order to lower the blanket temperature to the gas temperature. The flowrate was increased till the temperature, recorded by the thermocouple, reached a minimum value asymptotically. This closely corresponds to the gas temperature. To ensure that the flow profile inside the furnace was disturbed minimally, sampling was performed isokineticaly by adjusting the inlet cross sectional area of the suction thermometer. The suction thermometer was mounted on the motorized positioner described above and it was moved to various axial positions below the injector as well as three radial positions: at the centerline, close to the wall, and at half-distance in between.

Two sets of gas temperature data are shown in Fig. 5. It can be seen that, at the flow

conditions where most experiments are expected to take place, the gas temperature is fairly constant in the radiation cavity except under high injector velocities where the injector jet momentum dissipation is slow, as explained in the next section. Average gas temperatures are measured to be about 60-70 K lower than the wall temperatures.

**4 FLUID FLOW MODELLING** Efforts to study the high-temperature, gas-phase environment inside our experimental apparatus, the laminar flow, drop tube furnace were continued by employing numerical simulations. Various cases have been examined and an example is given below:

Results obtained with Fluent for two quite different cases are shown in Figs. 6a-c and 7a-c at furnace wall temperature, $T_w$, of 1500 K in the radiation cavity, main furnace flow rate of 2 lpm and for injector flow rates of 0.1 lpm (Fig. 6) and 1.0 lpm (Fig. 7). $T_w$ at the regions were the top and bottom insulation sections exist was assumed to increase (decrease) according to linear ramp profiles. The entering temperature of air at the second flow straightener was set to 800 K in this case extrapolating from measurements made elsewhere. In all of these plots the scale in the radial direction has been expanded by 2.5 times. Figs. 6a or 7a, and 6b or 7b depict the velocity profiles in the axial and radial direction, respectively. In Fig. 6c or 7c temperature profiles are depicted. Contrasting these two cases it can be seen how widely the injector air stream can influence the flow conditions inside the furnace. Under these conditions it takes a length of about 2 injector inner diameters for the momentum of the jet to dissipate. for the first case but it never dissipates (in the length of our furnace) in the second case. Again the highest velocities are observed to take place below the exit of the injector. It can also be observed that it takes ca. 6 injector diameters, in the first case, or over 22 injector diameters, in the second case, for the entering gas temperature to climb to values close to $T_w$. Many different cases have been investigated for furnace flowrates varying between 1 to 2 lpm, injector flowrates between 0.0 and 1.0 lpm, at three wall temperatures: 1150, 1500 and 1850 K. Results are plotted on Figs. 8-11. Figures 8 and 9 illustrate the effects of the injector flowrate on the axial velocity and temperature profiles, respectively. For all these cases the calculated average velocities in the furnace were in the range of 5 to 10 cm/s. Low

injector flow rates result in local centerline velocities that do not deviate much from the average velocities, meanwhile injector flowrates of 0.5 to 1.0 result in centerline velocities that are up to 7 times higher than the calculated average. This was a rather unexpected result. Similar trends are noticed in the temperature profiles (Fig. 9). This suggests that the injector flowrates should be kept to the neighborhood of 0.1 lpm if fairly uniform velocity and gas temperature profiles are desired under these conditions.

The effects of the furnace flowrate on the centerline temperature were minimal as shown in Fig. 10. The effects of the axial position of the flow straightener were also found to be unimportant and moving the flow straightener closer to the injector tip did not seem to influence either the velocity or the temperature profiles in the furnace.

The effect of the wall temperature on the gas temperature is also shown in Fig. 11 where the difference between the furnace maximum wall temperature, MWT, and the centerline temperature $T_c$ is plotted for the case of an injector flow rate of 0.5 lpm. The largest temperature gradients are experienced at the highest wall temperatures and it takes six injector diameters for the centerline to heat to within 200 K from the wall temperature. The corresponding distance for the case of an injector flow rate of 0.1 lpm is one injector diameter only , Fig. 11.

## 4 COMPARISON OF CALCULATED AND MEASURED TEMPERATURE PROFILES

Calculated temperature profiles, along the centerline of the furnace, have been contrasted to experimental values obtained using the suction pyrometer; the results are shown in Figs. 12-16. Results obtained at a maximum wall temperature of 1500 K are depicted in Figs. 12-14; the furnace flow rate was set to 2.0 lpm and the injector flow rate was varied from 0.1 lpm (Fig. 12) to 0.5 lpm (Fig. 13) to 1.0 lpm (Fig. 14). Similar results obtained at a wall temperature of 1850 K and are depicted in Figs. 15-16. Observing the experimentally obtained profiles it can be seen that the maximum centerline gas temperatures are 60-70 K below the maximum w all temperature, also within the first 2-3 cm below the injector tip the gas temperature is substantially lower (200-300 K) than the wall. This trend becomes

more pronounced at the highest flow rate (1 lpm) where in the first 7 cm the gas temperatures are up to 400 K below the wall. The numerical results appear to be very sensitive to the injector flow rate and even if at 0.1 lpm the calculate gas temperatures are above the experimental ones, at 0.5 lpm are below, and at 1.0 lpm are well below the experimental values. Trends at 1800 K are similar and the agreement between experimental and theoretical profiles are better.

**5 MODELLING THE EVAPORATION OF WATER DROPS** The fate of introduced water droplets in the furnace environment can also be modelled with the *Fluent* software package. The results are shown in Figs. 17a and 17b as two symmetric particle trajectories. In both cases the injector and furnace flowrates were set at 0.1 and 2.0 lpm, respectively and the wall temperature at 1500 K. Entering particle velocities were were set equal to terminal velocities by equating the aerodynamic drag forces equal to the gravity forces. Figure 17a shows the fate of a 50$\mu$m particle, which is seen to evaporate in 0.86 sec inside the water cooled injector. Figure 17b shows the lifetime of a 250 $\mu$m water drop which reached the radiation cavity and took an overall of 0.32 sec to evaporate. These results will be verified by an algorithm that is been currently developed.

## COAL-WATER SLURRY MIXING APPARATUS

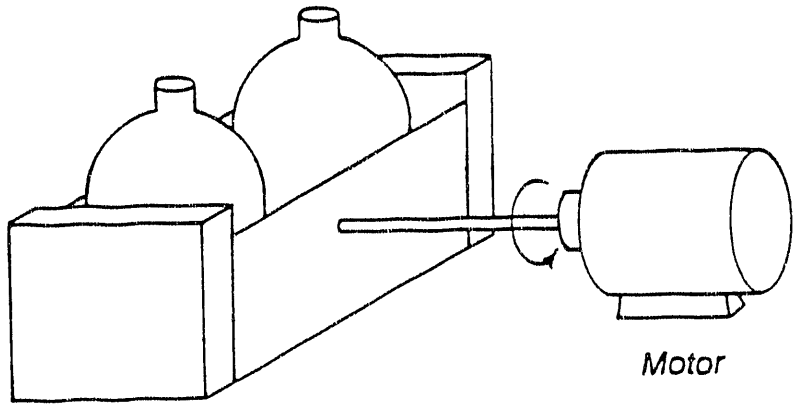


1. FIGURE 1. Schematic of the slurry tumbling apparatus.

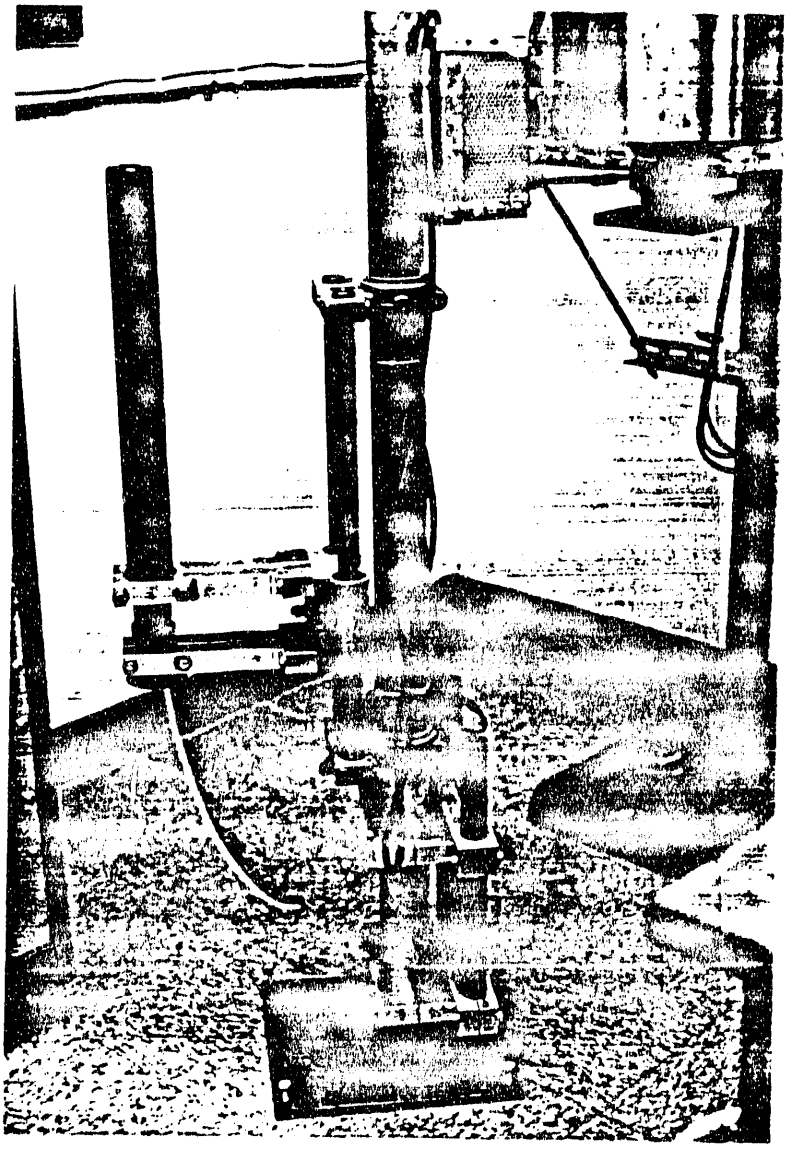

2. FIGURE 2. Photograph of the water-cooled, nitrogen flow, particle collection probe.

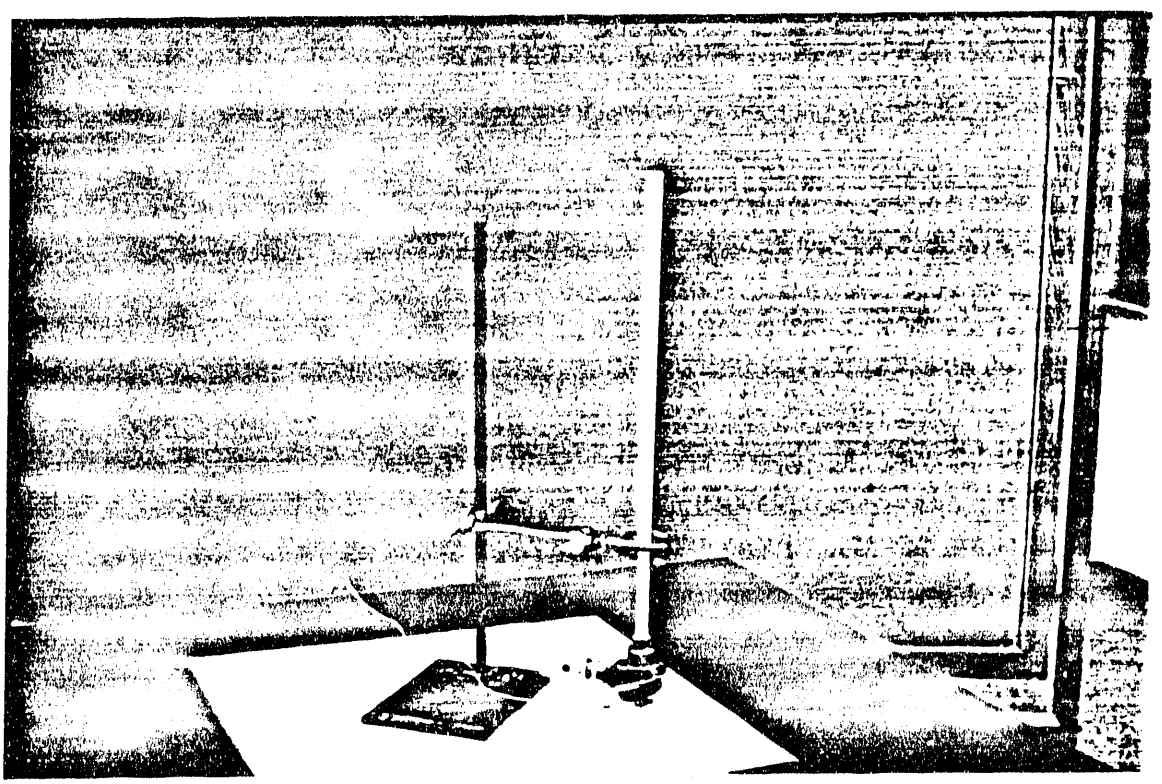

3. FIGURE 3. Photograph of the suction Thermometer.

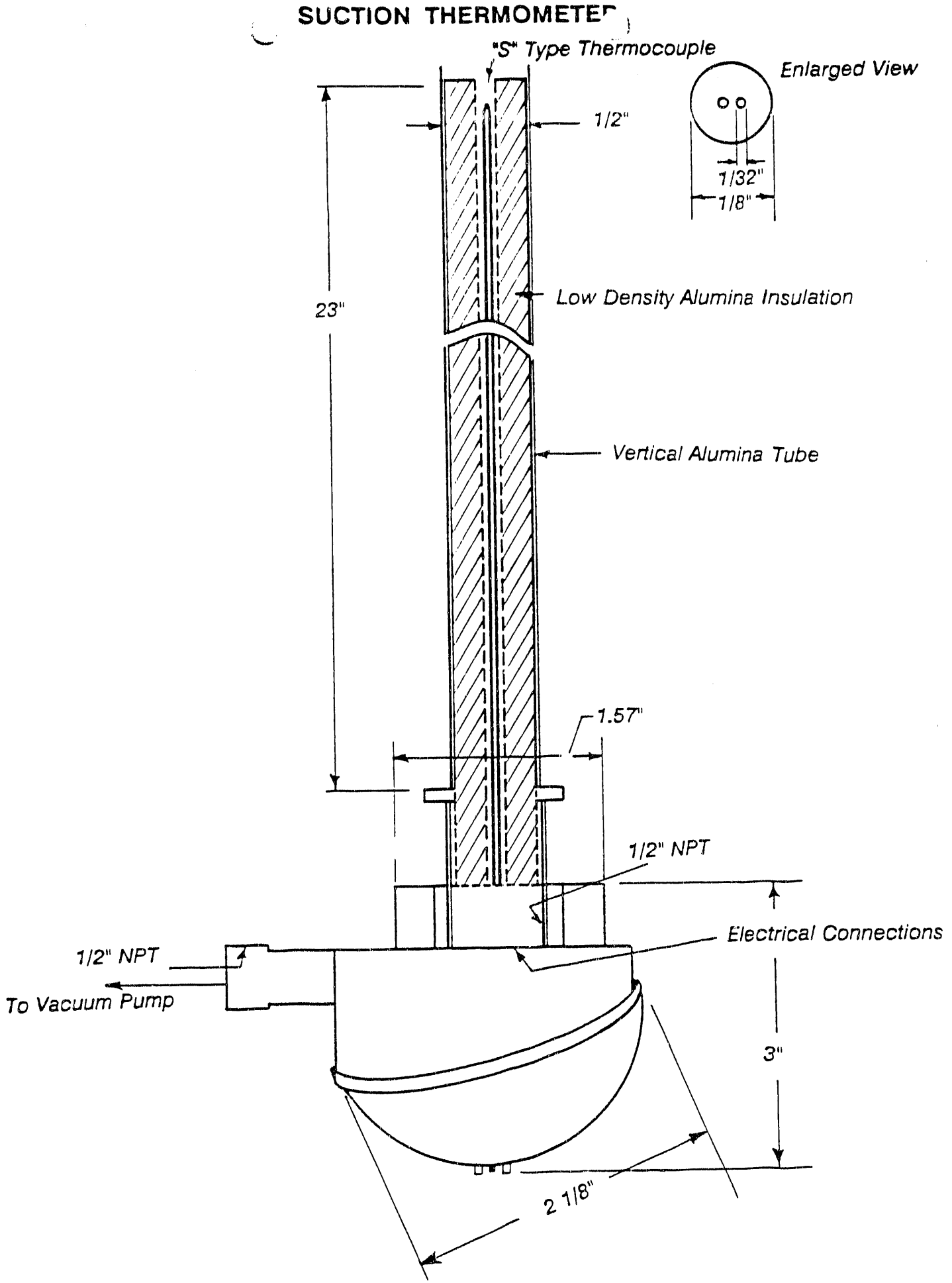


4. FIGURE 4. Schematic of the suction Thermometer.

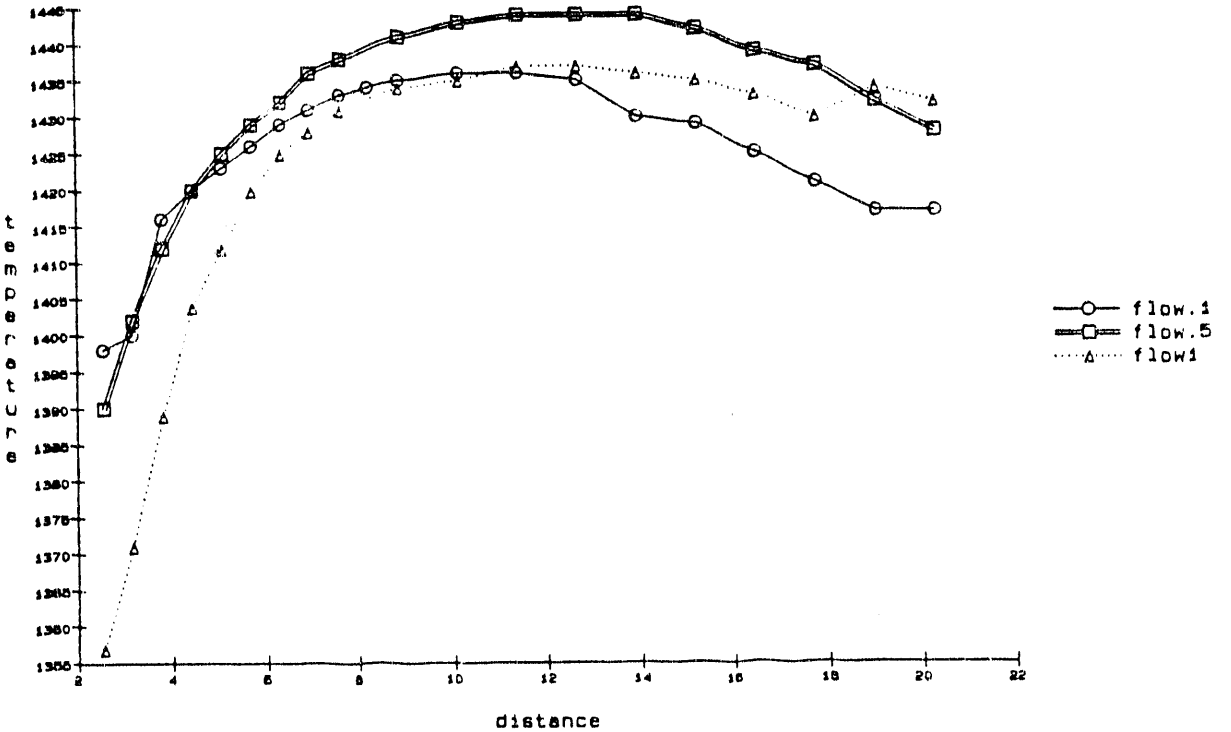


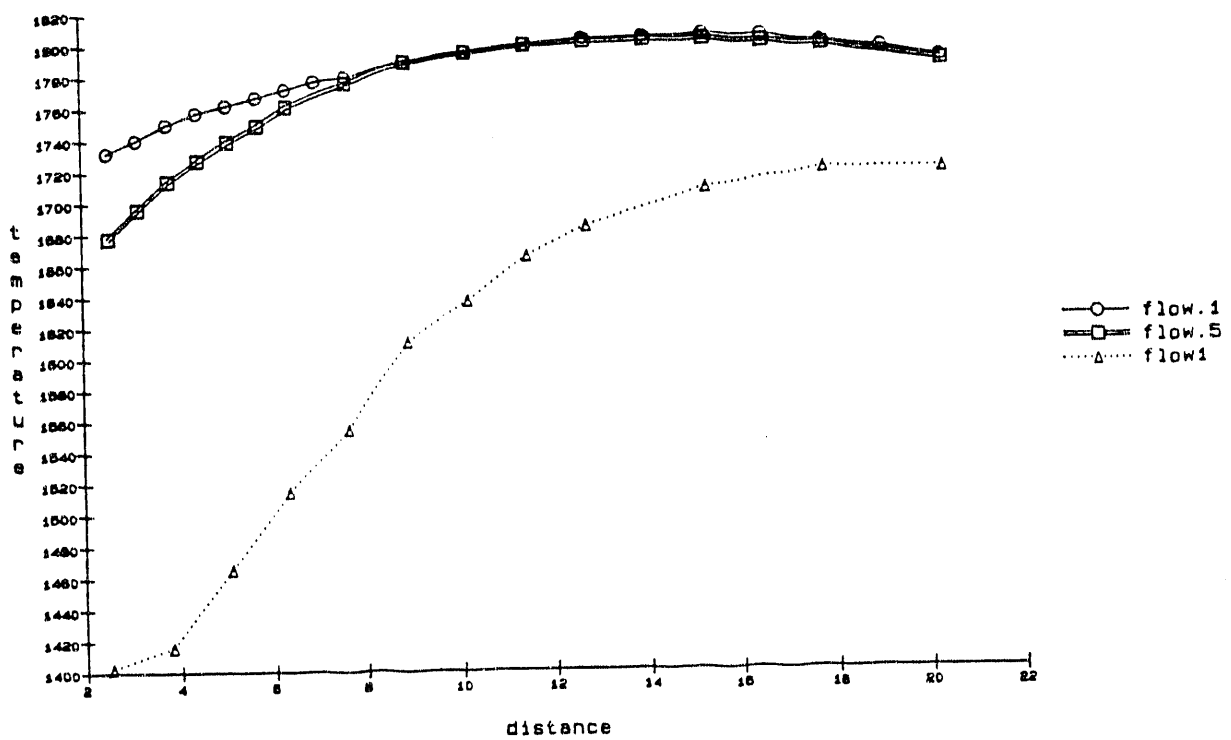


5. FIGURE 5. Gas temperature profiles along the centerline of the furnace, measured by suction thermometry.

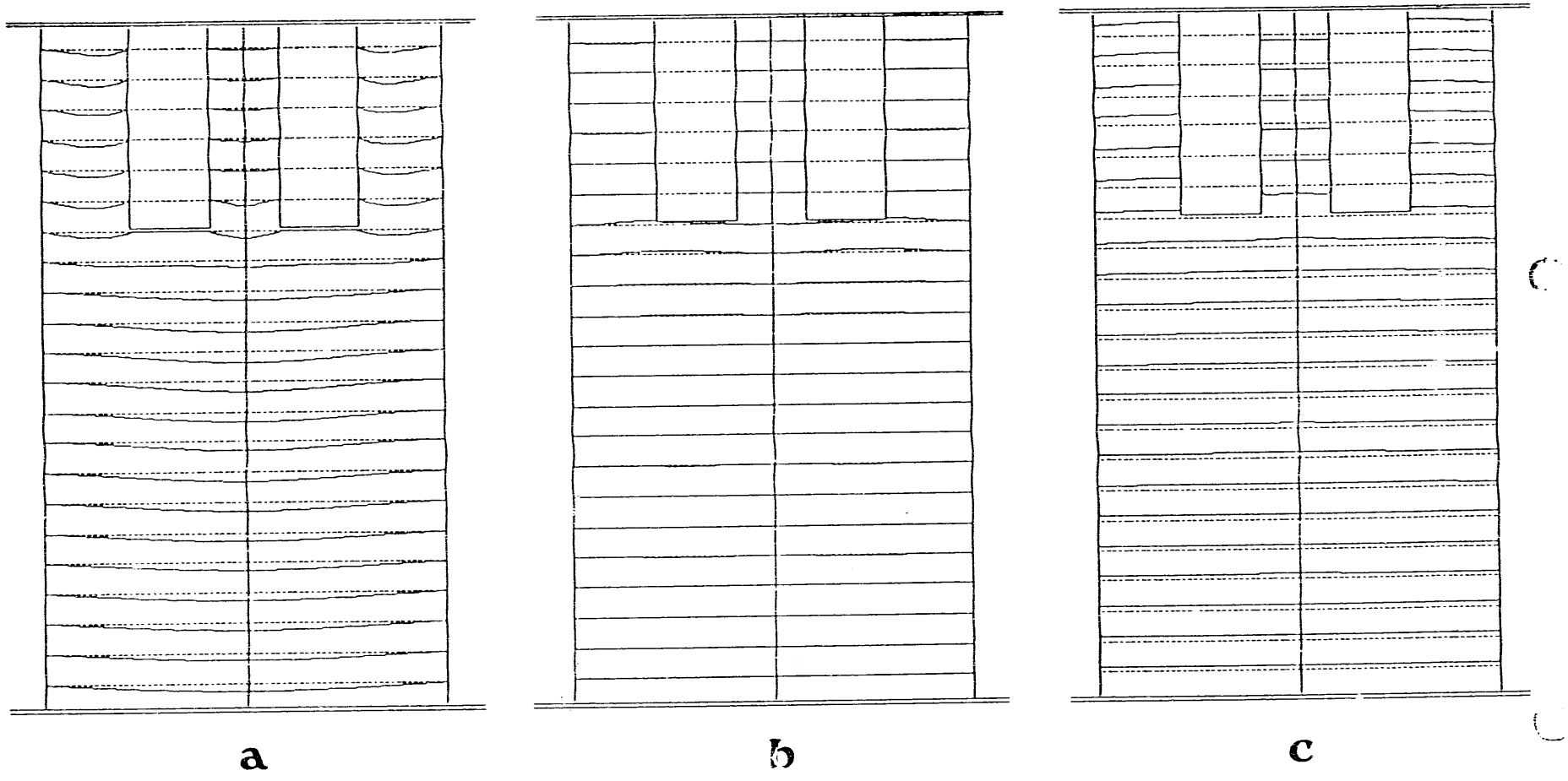


6. FIGURE 6. Numerical calculations for modelling the air flow inside the drop tube furnace, (i) vertical velocity profiles, (ii) radial velocity profiles, and (iii) temperature profiles. Conditions: furnace air flow-rate 2.0 lpm, injector flow-rate 0.1 lpm and $T_w$ = 1500 K.

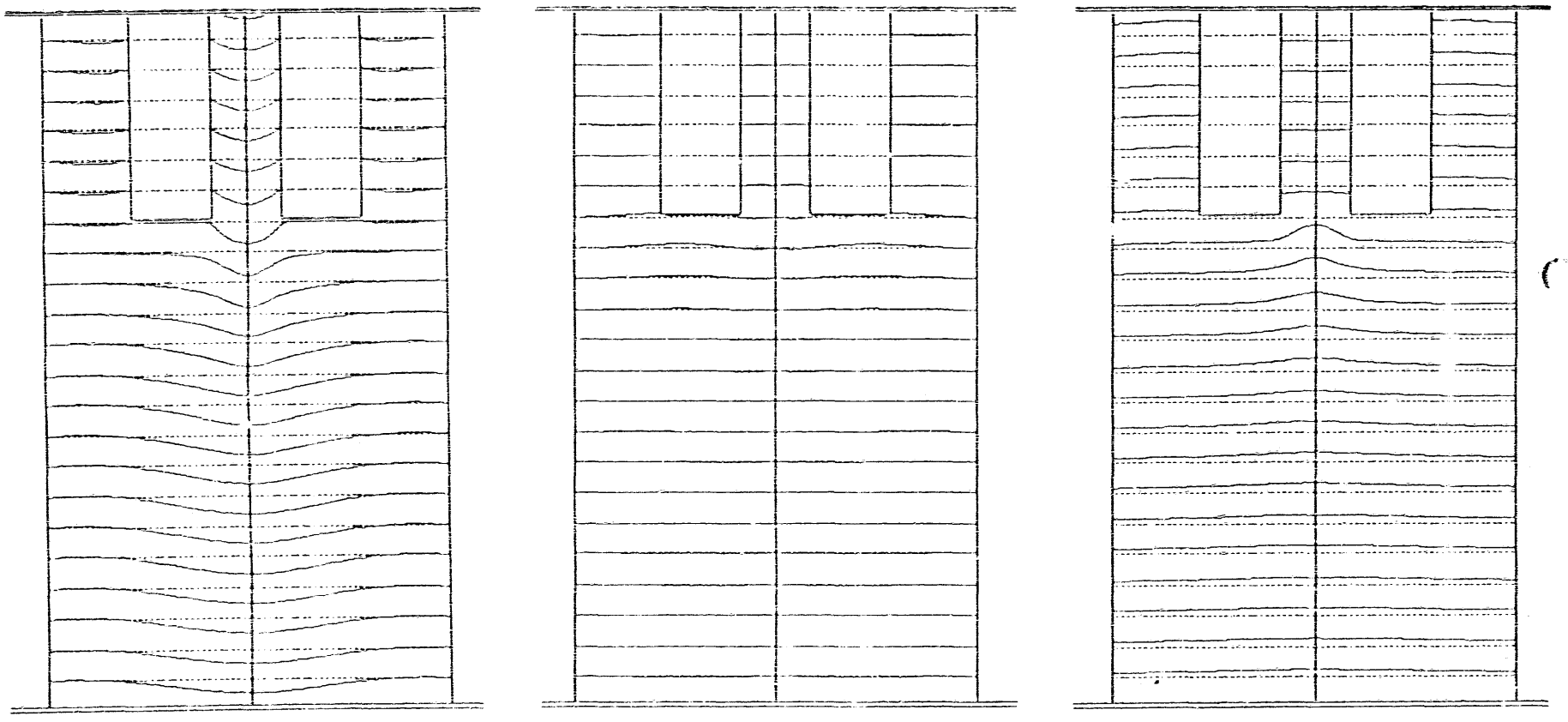


7. FIGURE 7. Numerical calculations for modelling the air flow inside the drop tube furnace, (i) vertical velocity profiles, (ii) radial velocity profiles, and (iii) temperature profiles. Conditions: furnace air flow-rate 2.0 lpm, injector flow-rate 1.0 lpm and $T_w$ = 1500 K.

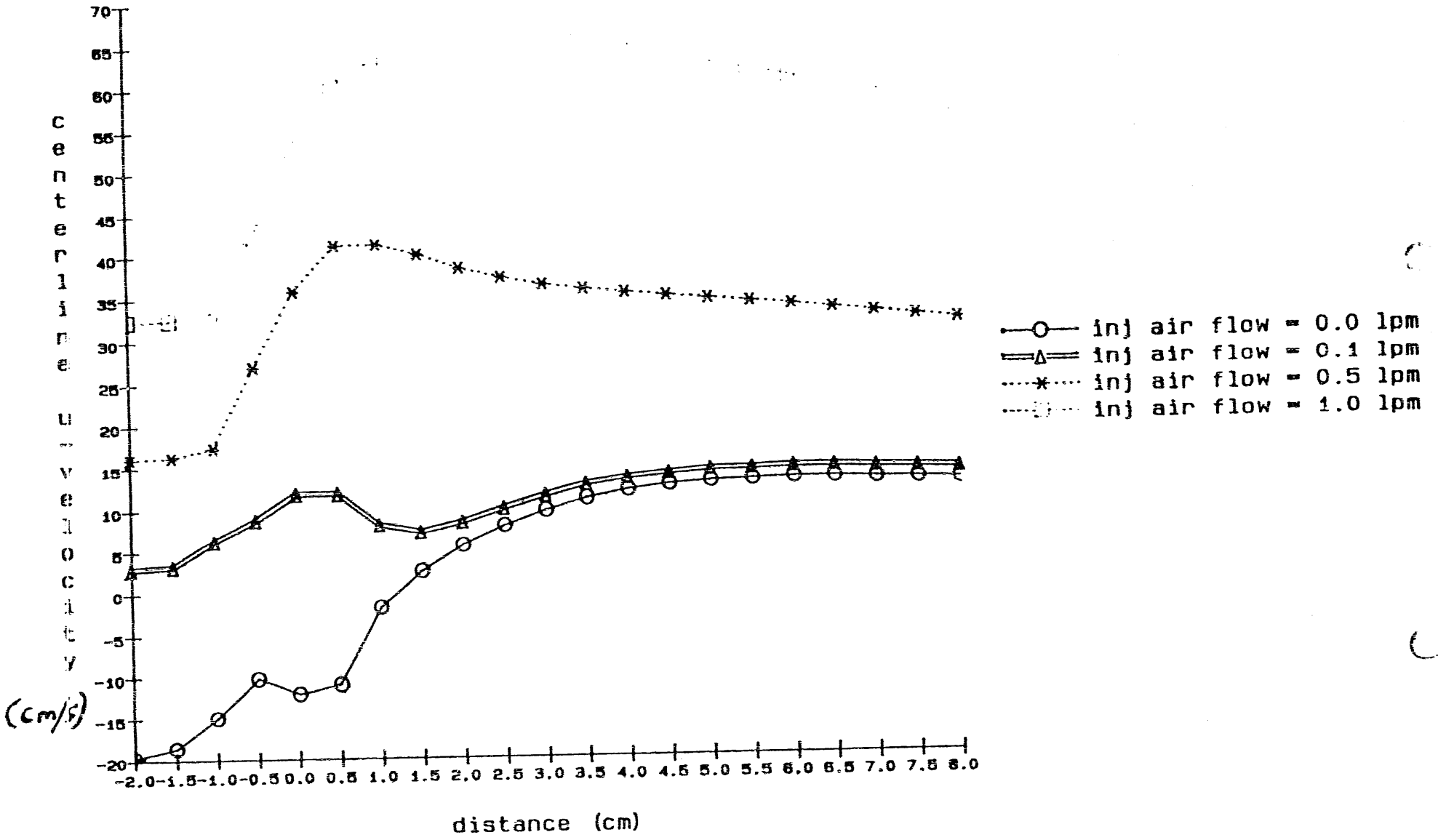


8. FIGURE 8. Numerical calculations of furnace centerline velocity vs. axial distance from the tip of the injector for four injector flowrates: 0.0, 0.1, 0.5, 1.0 lpm. Furnace flowrate at 2.0 lpm, wall temperature 1500 K.

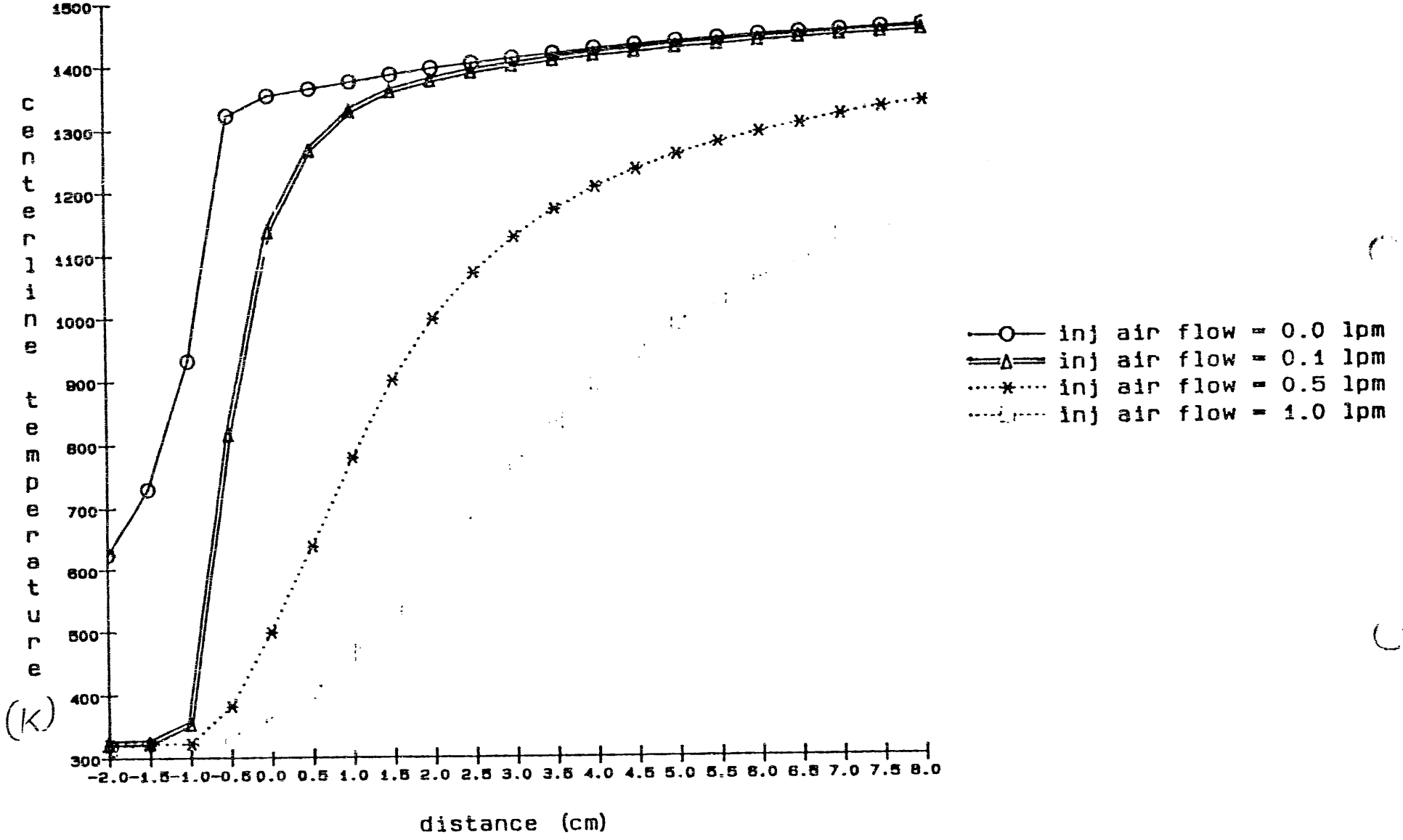


9. FIGURE 9. Numerical calculations of furnace centerline temperature vs. axial distance from the tip of the injector for four injector flowrates: 0.0, 0.1, 0.5, 1.0 lpm. Furnace flowrate at 2.0 lpm, wall temperature 1500 K.

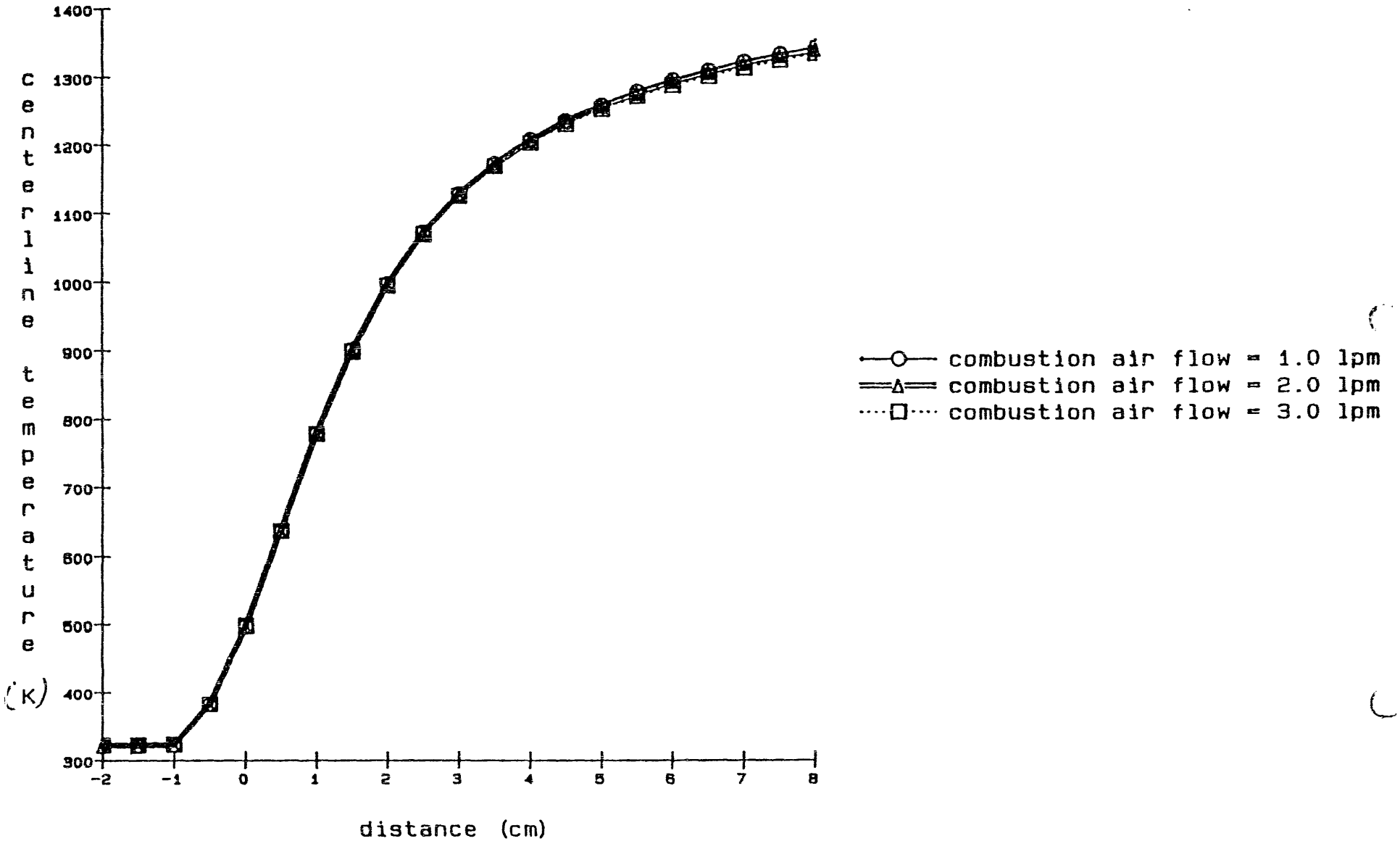


10. FIGURE 10. Numerical calculations of furnace centerline temperature vs. axial distance from the tip of the injector for three furnace flowrates: 1.0, 2.0, 3.0 lpm. Injector flowrate at 0.5 lpm, wall temperature 1500 K.

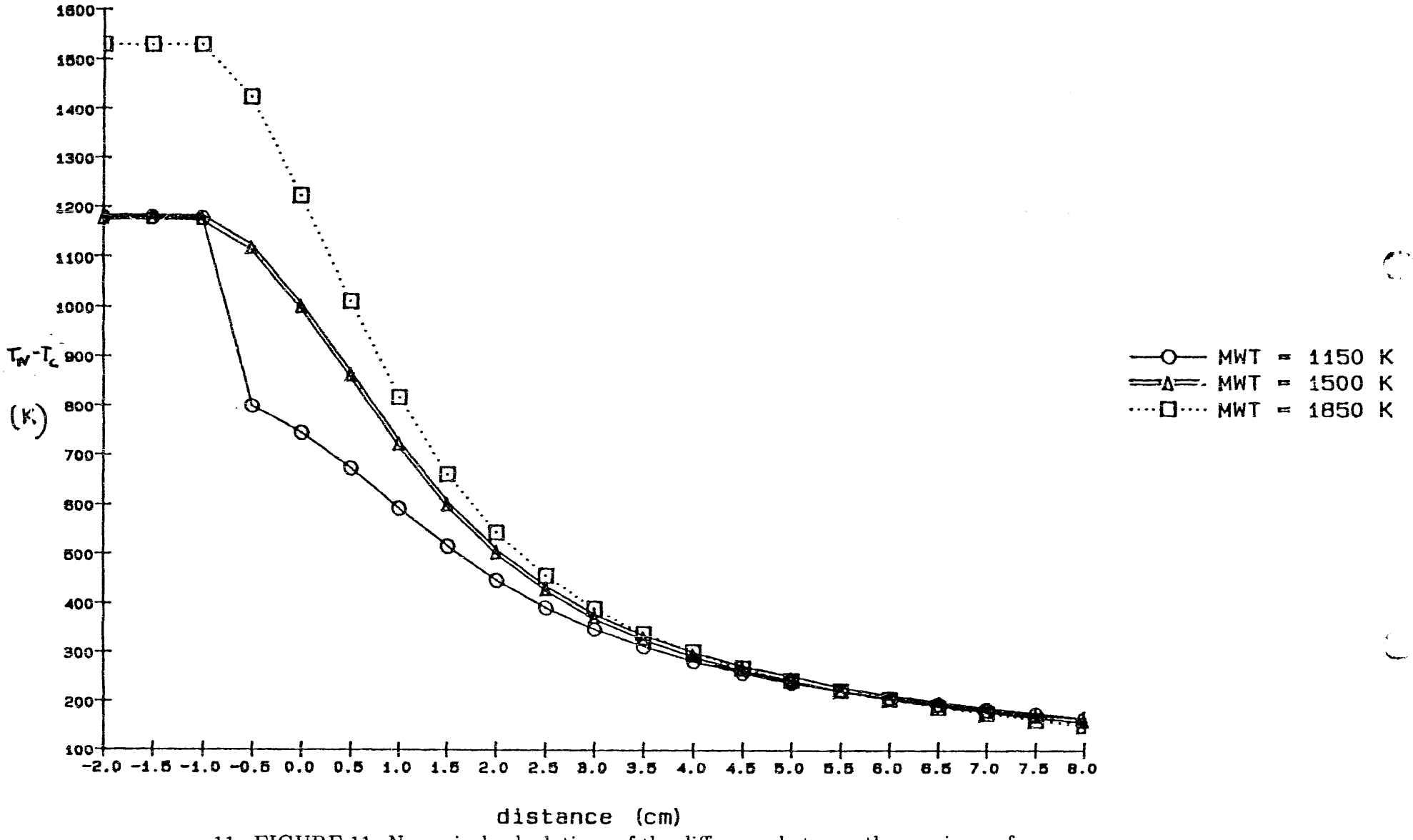


11. FIGURE 11. Numerical calculations of the difference between the maximum furnace wall temperature and the centerline temperature vs. axial distance from the tip of the injector for three wall temperatures 1150, 1500 and 1850 K. Furnace flowrate at 2.0 lpm, and injector flowrate at 0.5 lpm.

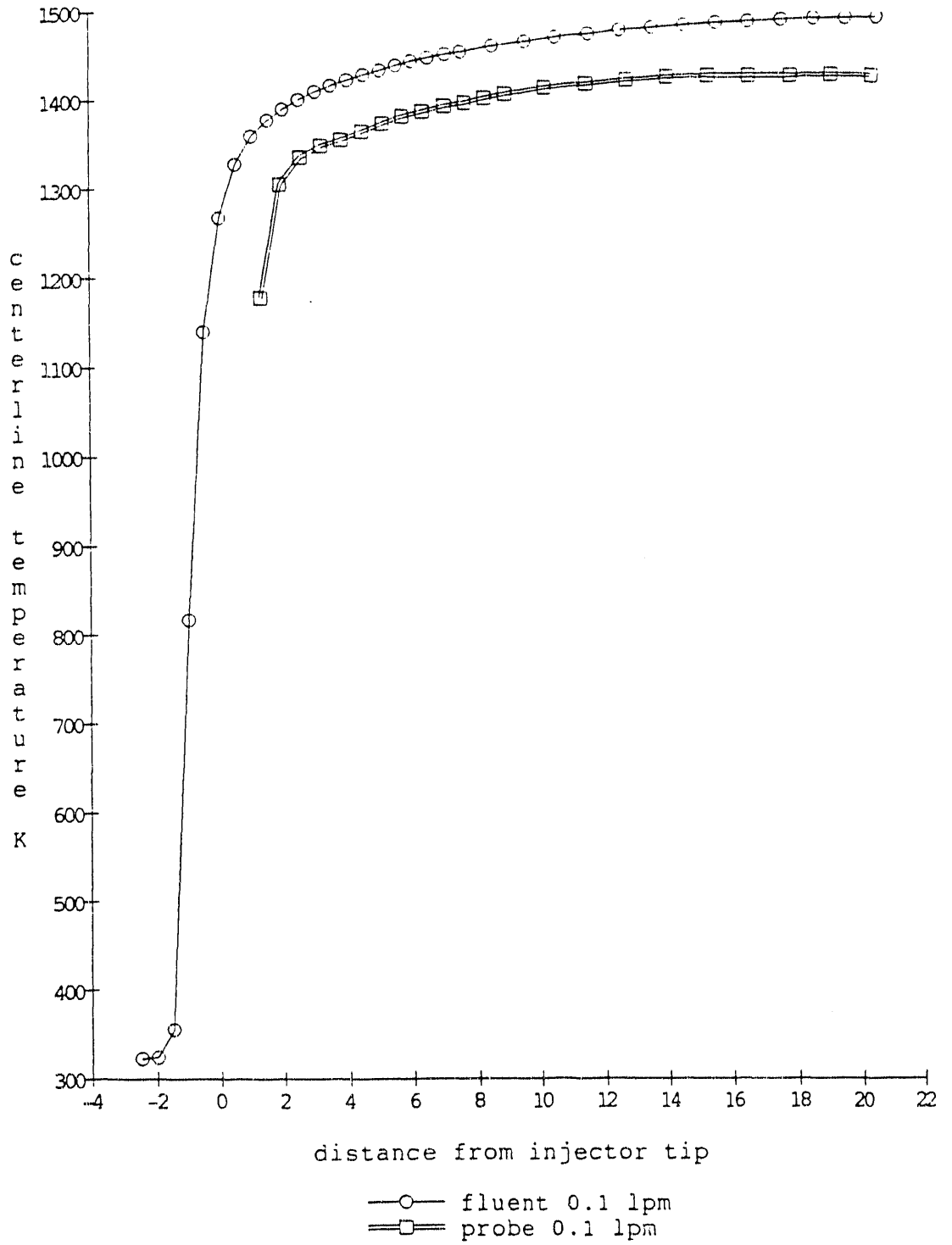


FIGURE 12. Comparison of experimental and theoretical temperature profiles at the centerline of the furnace. Injector flowrate at 0.1 lpm, furnace flowrate at 2.0 lpm, wall temperature 1500 K.

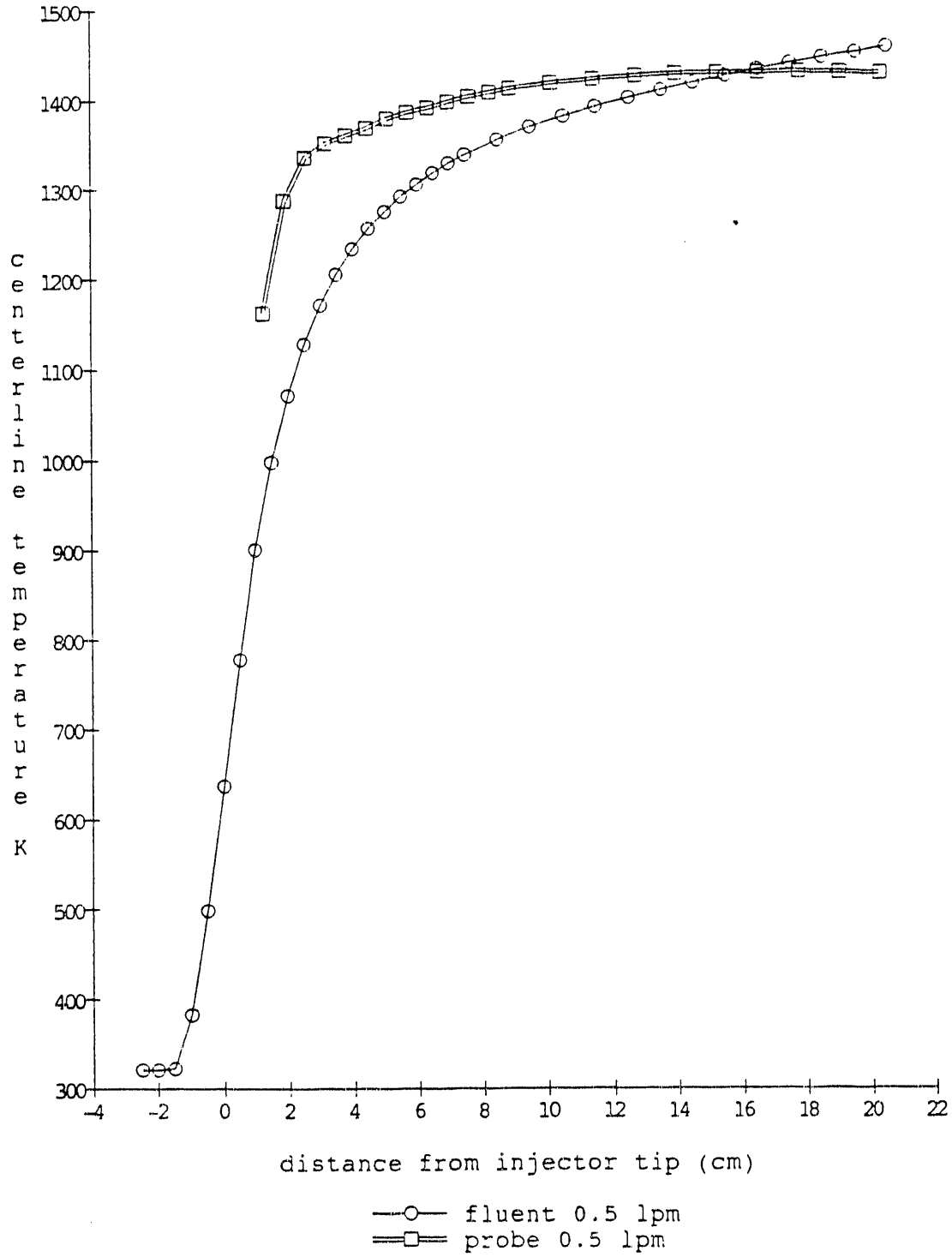


FIGURE 13. Comparison of experimental and theoretical temperature profiles at the centerline of the furnace. Injector flowrate at 0.5 lpm, furnace flowrate at 2.0 lpm, wall temperature 1500 K.

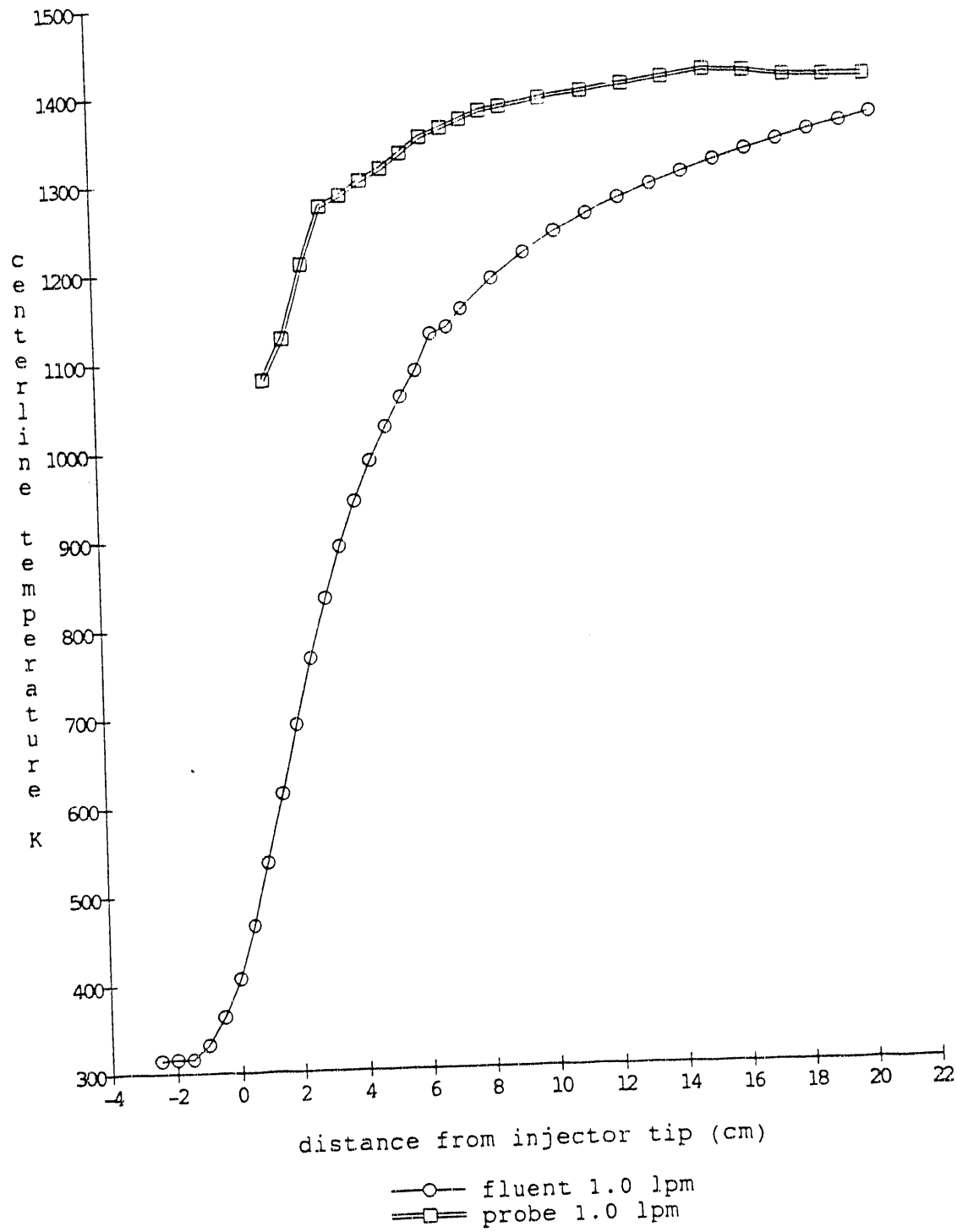


FIGURE 14. Comparison of experimental and theoretical temperature profiles at the centerline of the furnace. Injector flowrate at 1.0 lpm, furnace flowrate at 2.0 lpm, wall temperature 1500 K.

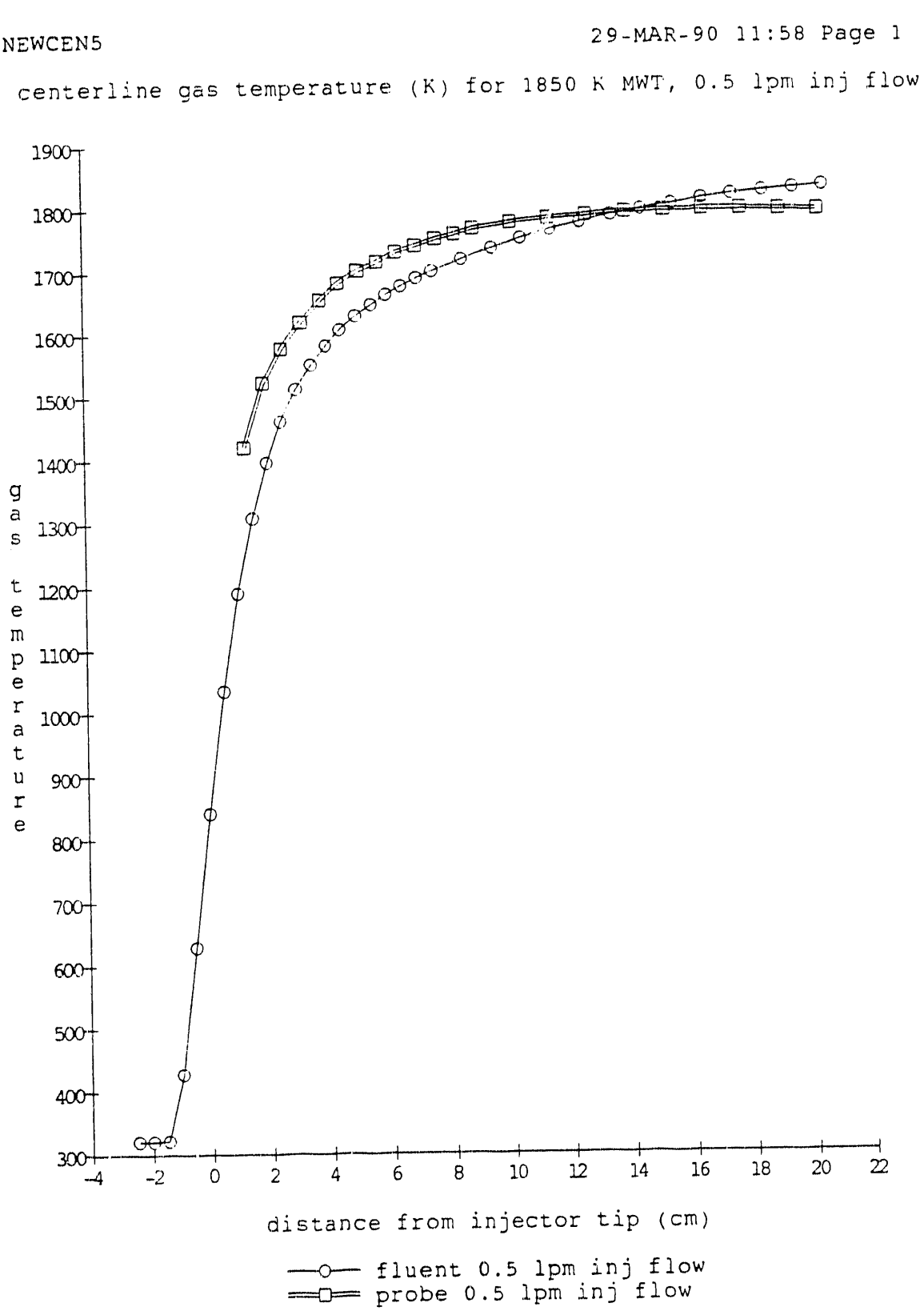


FIGURE 15. Comparison of experimental and theoretical temperature profiles at the centerline of the furnace. Injector flowrate at 0.1 lpm, furnace flowrate at 2.0 lpm, wall temperature 1850 K.

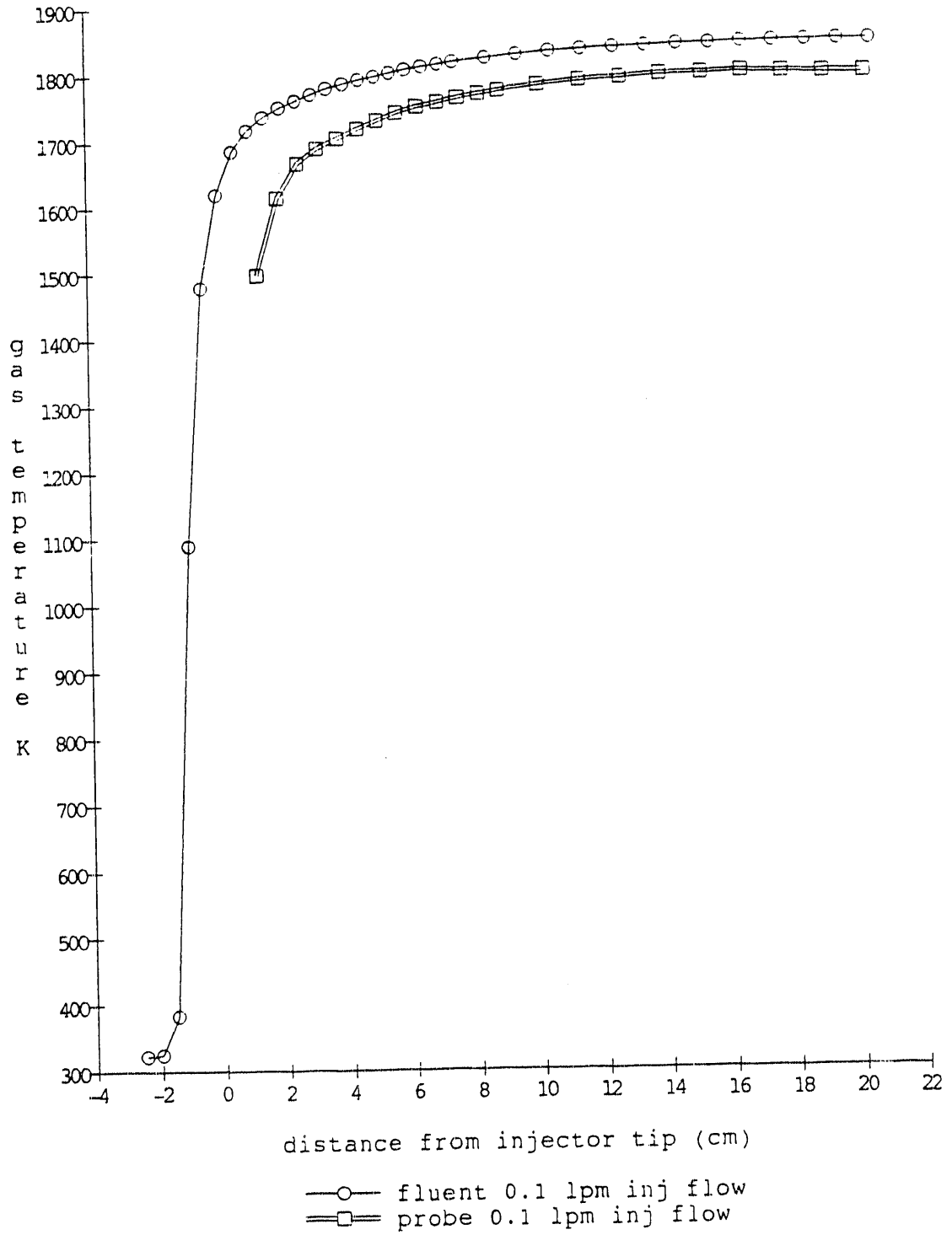


FIGURE 16. Comparison of experimental and theoretical temperature profiles at the centerline of the furnace. Injector flowrate at 0.5 lpm, furnace flowrate at 2.0 lpm, wall temperature 1850 K.

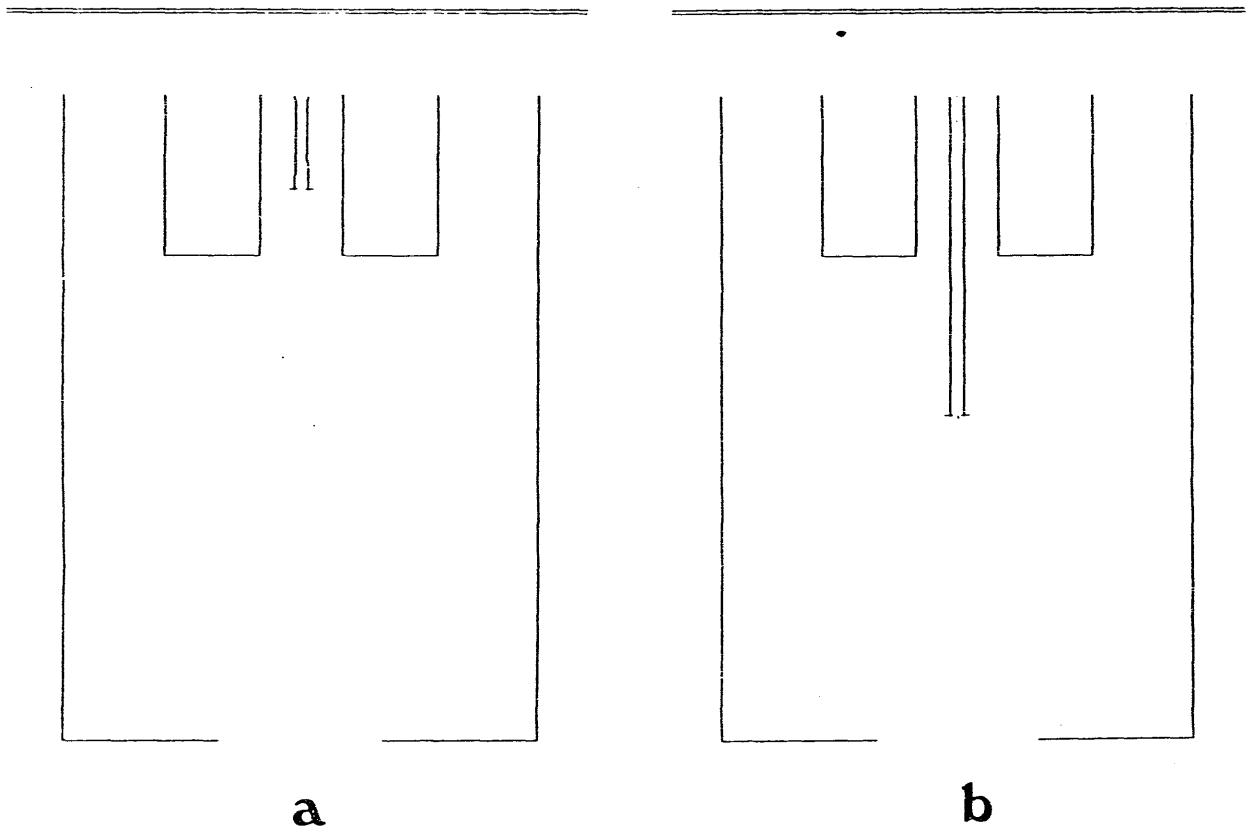


17. FIGURE 17. Numerical calculations of trajectories of evaporating water drops of 50$\mu$m and 250$\mu$m water drops. Injector flowrates at 0.1 lpm, furnace flowrate at 2.0 lpm, wall temperature 1500 K.

# END

DATE
FILMED
9/04/92